Biomaterials 273 (2021) 120815

Contents lists available at ScienceDirect

Biomaterials

journal homepage: www.elsevier.com/locate/biomaterials

In vivo remodeling of human cell-assembled extracellular matrix yarns

Laure Magnan [a], Fabien Kawecki [a], Gaëlle Labrunie [a], Maude Gluais [a], Julien Izotte [b], Sébastien Marais [c], Marie-Pierre Foulc [d], Mickaël Lafourcade [d], Nicolas L'Heureux [a,*]

[a] Univ. Bordeaux, INSERM, BIOTIS, UMR1026, F-33000, Bordeaux, France
[b] Animal Facility A2, University of Bordeaux, F-33076, Bordeaux, France
[c] UMS 3420 CNRS, US4 INSERM, Bordeaux Imaging Center, University of Bordeaux, F-33000, Bordeaux, France
[d] Rescoll Société de Recherche, 8 Allée Geoffroy Saint-Hilaire, CS 30021, F-33615, Pessac, France

ARTICLE INFO

Keywords:
Tissue-engineered yarn
Cell-assembled extracellular matrix
Inflammatory response
In vivo remodeling
Mechanical properties
Human textiles

ABSTRACT

Cell-assembled extracellular matrix (CAM) has been used to produce vascular grafts. While these completely biological vascular grafts performed well in clinical trials, the *in vivo* remodeling and inflammatory response of this truly "bio" material has not yet been investigated. In this study, human CAM yarns were implanted subcutaneously in nude rats to investigate the innate immune response to this matrix. The impact of processing steps relevant to yarn manufacturing was evaluated (devitalization, decellularization, gamma sterilization, and twisting). We observed that yarns were still present after six months, and were integrated into a non-inflamed loose connective tissue. The CAM was repopulated by fibroblastic cells and blood vessels. While other yarns caused minor peripheral inflammation at an early stage (two weeks of implantation), gamma sterilization triggered a more intense host response dominated by the presence of M1 macrophages. The inflammatory response was resolved at six months. Yarn mechanical strength was decreased two weeks after implantation except for the more compact "twisted" yarn. While the strength of other yarns was stable after initial remodeling, the gamma-sterilized yarn continued to lose mechanical strength over time and was weaker than devitalized (control) yarns at six months. This is the first study to formally demonstrate that devitalized human CAM is very long-lived *in vivo* and does not trigger a degradative response, but rather is very slowly remodeled. This data supports a strategy to produce human textiles from CAM yarn for regenerative medicine applications where a scaffold with low inflammation and long-term mechanical properties are critical.

1. Introduction

Over the past ten years, vascular tissue engineering has flourished with two approaches to produce arterial bypass grafts reaching clinical trials [1,2]. We pioneered the use of cell-assembled extracellular matrix (CAM) synthesized *in vitro* by human skin fibroblasts as a robust biological scaffold to produce vascular grafts without exogenous materials [3,4]. Living and autologous blood vessels constructed by rolling sheets of CAM were the first tissue-engineered vascular grafts (TEVGs) to be implanted in the human arterial circulation [1,5]. Moreover, allogeneic TEVGs, that were devitalized by a simple dehydration process, have been implanted in patients without signs of rejection, which opened the door to an "off-the-shelf" approach for vascular tissue engineering [6]. While CAM-based vascular grafts rapidly reached the clinic with successful outcomes, the *in vivo* remodeling of this "bio" material has not been carefully studied. Indeed, the grafts were rarely retrieved during the clinical trial because TEVGs were implanted as arteriovenous shunts in complex patients with multiple comorbidities. Furthermore, the intense inflammatory environment of a failed arteriovenous shunt, which was punctured three times per week with two large-bore needles, likely masked the body's normal remodeling response to the CAM tissue.

The production of TEVGs by rolling sheets of CAM requires a first step of culture within sterile flasks (approximately ten weeks) followed by a period of maturation (approximately ten additional weeks) using a bioreactor to fuse the various layers of the blood vessel [1,3–7]. In order to provide a much faster and economical production strategy, we recently developed TEVGs using a textile approach [8]. Biological yarns were produced by cutting strips of CAM to obtain "ribbons", which could be further processed into "threads" by twisting them. These yarns (ribbons or threads) can be devitalized by a simple dehydration process and

* Corresponding author. BIOTIS – Laboratory for the Bioengineering of Tissues (UMR Inserm 1026), University of Bordeaux, Campus Carreire, 146 Rue Léo-Saignat, case 45, Bordeaux Cedex, 33077, France.
E-mail address: Nicolas.lheureux@inserm.fr (N. L'Heureux).

https://doi.org/10.1016/j.biomaterials.2021.120815
Received 30 November 2020; Received in revised form 3 April 2021; Accepted 6 April 2021
Available online 14 April 2021

stored dry until needed. By weaving this human yarn, devitalized TEVGs with impressive mechanical strength can be produced in a few days. This approach could be readily automated, which would further significantly reduce production time (cost) and improve the quality and the reproducibility of the textile.

In this study, we analyzed the *in vivo* remodeling of the devitalized CAM in a controlled environment using a simple implant (a yarn), which allowed for both straightforward histological and mechanical evaluations. In addition, we examined whether different processing steps that are relevant to the manufacturing of an implantable textile, such as decellularization, gamma sterilization, or twisting, would adversely affect yarn integrity or its *in vivo* remodeling. Therefore, processed human yarns were subcutaneously implanted in athymic nude rats for up to six months. This well-established animal model allowed the evaluation of the innate immune response without interference from the adaptive immune system that would reject the human tissue [9]. Evaluating the responses to these yarns will indicate which processing approaches are acceptable for the manufacturing of a woven TEVG or other human textiles.

2. Materials and methods

2.1. Human skin fibroblast culture and CAM production

Human skin fibroblast cells (HSFs) were isolated from healthy adult patients according to our previously described protocol [4]. The HSFs were grown in Dulbecco's modified Eagle medium containing F-12 nutrient mixture (DMEM/F-12; 31331-028; Gibco®, ThermoFisher Scientific, Bordeaux, France) supplemented with 20% fetal bovine serum (FBS) (Hyclone SH30109.03, GE Healthcare Life Science, Washington, WA, USA) in humidified 37 °C incubators with 5% CO_2 and frozen at the end of the 3rd passage. For the production of the CAM, frozen cells were thawed in passage 4 (P4) and cultured for one week. HSFs were seeded at a density of 1×10^4 cell/cm^2 (P5) in 225 cm^2 flasks and cultured for approximately eight weeks in medium supplemented with 500 μM of sodium L-ascorbate (A4034-500G; Sigma-Aldrich, Saint-Quentin-Fallavier, France). The media was changed three times per week.

2.2. CAM devitalization

CAM sheets were quickly rinsed in sterile distilled water and frozen at −80 °C. Sheets were then thawed, quickly rinsed in sterile distilled water, air-dried under the sterile flow of a biosafety cabinet at room temperature for at least 2 h, and stored at −80 °C until needed. For yarn production, sheets were rehydrated in water, cut to desired dimensions, and air-dried under the sterile flow of a biosafety cabinet at room temperature for at least 2 h. Dry CAM yarns were spooled and stored at −80 °C.

2.3. CAM decellularization

The decellularization process was realized on devitalized CAM sheets. CAM sheets, devitalized as described in section 2.2, were rehydrated using sterile distilled water for at least 1 h. The water was then replaced with 150 mL of a decellularization solution composed of 8 mM 3-[(3-cholamidopropyl)dimethylammonio]-1-propanesulfonate (CHAPS; Sigma-Aldrich, Saint-Quentin-Fallavier, France), 1000 mM sodium chloride (NaCl; S9888-1 KG; Sigma-Aldrich, Saint-Quentin-Fallavier, France), 25 mM ethylenediaminetetraacetic acid (EDTA; EDS-1KG; Sigma-Aldrich, Saint-Quentin-Fallavier, France), and 120 mM sodium hydroxide (NaOH; 30620-1 KG; Sigma-Aldrich, Saint-Quentin-Fallavier, France) diluted in 1X phosphate buffer saline (1X PBS; 10010023; Gibco®, ThermoFisher Scientific, Bordeaux, France). The CAMs were treated for 6 h under intense rocking agitation. Then, the CAM sheets were rinsed three times in 1X PBS for 30 min and once in sterile distilled water overnight under agitation. Finally, the decellularized CAM tissues were stored in sterile distilled water at 4 °C for 24 h before being processed for nucleus imaging, histology, or production of decellularized yarns.

2.4. Production of devitalized, decellularized, and twisted yarns

Yarns were produced as previously described [8]. CAM sheets were placed on a sterilized custom cutting device. A series of circular blades, separated by 5-mm spacers, was pressed and rolled on the sheet to produce ribbons (16- to 18-cm long). Ribbon yarns were subsequently dried under sterile condition, individually spooled around sterile supports, placed in sterile tubes, and stored at −80 °C. To produce twisted yarn (threads), one extremity of the rehydrated ribbon was attached to the rotating rod of a custom twisting device, while a manipulator pinched the other extremity. The calibrated motor was turned on for a calculated duration to twist the ribbons at 7.5 revolutions per cm of length, while the manipulator manually massaged the yarn.

2.5. Gamma sterilization of the devitalized yarns

Gamma sterilization was performed on spooled devitalized yarns that were previously dried. They were taken out of the −80 °C freezer and shipped in tubes, at ambient temperature, to the company Steris (Marcoule, France). They were exposed for 3 h and received a 25 kGy irradiation dose generated by a source of ^{60}Cobalt.

2.6. Subcutaneous implantation of the yarns in nude rats

Nude rats were anesthetized using isoflurane gas, and incision sites were disinfected with ethanol. Small punctures were made in the skin, at shoulder level and on the lower back, with a 18G needle. Devitalized, decellularized, gamma sterilized, and twisted yarns (rehydrated with sterile 1X PBS) were inserted in the eye of a sterile 17-cm long needle. Four yarns were implanted per rat. Three-mm wide ribbons of a clinically used membrane of processed bovine collagen (BioMend®; 0107; Zimmer Biomet Dental, Rungis, France) were used as a positive control to prove that the innate immune system of the nude rats was functional. After implantation, antibiotics were sprayed at the incisions sites. Samples were explanted at two weeks, as well as one, three, and six months after implantation. Eight samples per condition per time point were implanted into two animals (n = 8 grafts/condition/time point). All procedures and animal treatments complied with the principles of laboratory animal care formulated by the national society for medical research. This study was carried out in an accredited animal facility and was approved by the animal ethics committee of the University of Bordeaux.

2.7. Histological analyses

Samples were fixed overnight in 4% paraformaldehyde (PFA), rinsed, dehydrated, and paraffin-embedded. Seven-μm-thick paraffin-embedded sample sections were colored with Hematoxylin-Eosin staining (H&E). Images were captured using a NanoZoomer S60 digital slide scanner (C13210-01; Hamamatsu; Massy, France).

2.8. Indirect immunofluorescent staining against matrix proteins

Samples were fixed in 4% PFA overnight. After two rinses in 1X PBS, samples were dehydrated and embedded in paraffin. Paraffin sections (7 μm) were deparaffinized in toluene, followed by a descending series of ethanol, and those were processed for immunofluorescent staining. Deparaffinized sections were pretreated with citrate (pH 6.0) for 20 min at 95 °C and then washed with 1X PBS. Samples were immersed in blocking solution (3% goat normal serum diluted in 1X PBS) for 30 min at room temperature. Then, samples were incubated overnight at 4 °C with rabbit polyclonal primary antibodies against either collagen-I

(ab34710; Abcam, Cambridge, UK), fibronectin (ab23750; Abcam), or thrombospondin (ab85762; Abcam) diluted in blocking solution (1:200). Negative controls received blocking solution only. Following a washing step, the secondary antibodies Alexa Fluor 568-conjugated goat anti-rabbit (1:300; A-11036; Invitrogen, Barcelona, Spain) and 4′,6-diamidino-2-phenylindole (DAPI; 1:1000; D1306; Invitrogen) were applied for 2 h at room temperature. Images were acquired using a confocal microscope (TCS SPE, Leica microsystems, Wetzlar, Germany).

2.9. M1/M2 macrophages imaging and quantification

Inflammation generated by the presence of the yarns was quantified at two weeks, as well as one, three, and six months after implantation. Explanted samples of the yarns were processed as described in section 2.8 for M1/M2 immunostaining. M1 cells were double-stained with rabbit polyclonal antibodies against CCR7 (1:100; ab32527; Abcam) and mouse polyclonal antibodies against CD68 (1:100; ab31630; Abcam). M2 cells were double-stained with rabbit polyclonal antibodies against CD206 (1:100; ab64693; Abcam) and mouse polyclonal antibodies against CD68 (1:100; ab31630; Abcam). Secondary antibodies Alexa Fluor 568-conjugated goat anti-rabbit (A-11036; Invitrogen) and Alexa Fluor 488-conjugated goat anti-mouse (A-11001; Invitrogen) were diluted (1:300) in the presence of DAPI (1:1000) and applied for 2 h at room temperature. Images were acquired using a confocal microscope (TCS SPE, Leica microsystems). Quantification of M1 cells (CD68 and CCR7 positive cells) and M2 cells (CD68 and CD206 positive cells) was performed using a macro in ImageJ® software (NIH, Bethesda, MD, USA). Briefly, the yellow signal (double staining green and red) was isolated (threshold) and particles of the approximate size of a macrophage (five pixels and beyond) were counted in a 100-μm wide band surrounding the yarn. (n = 2–3 representative yarns/condition/time point).

2.10. Mechanical characterization of the yarns

Yarn diameters were measured using a biaxial laser micrometer (XLS13XY; Xactum; AEROEL; Pradamano, Italy). Then, yarns were clamped in the jaws of a tensile testing machine (Criterion® 43; MTS; Berlin, Germany) equipped with a 250 N force sensor, pre-stretched at 20 mm/min until reaching 0.1 N and pulled until rupture. The ultimate tensile stress (UTS) was calculated from the maximum force recorded during the test divided by the cross sectional area. (n = 4–15 yarns/condition/time point).

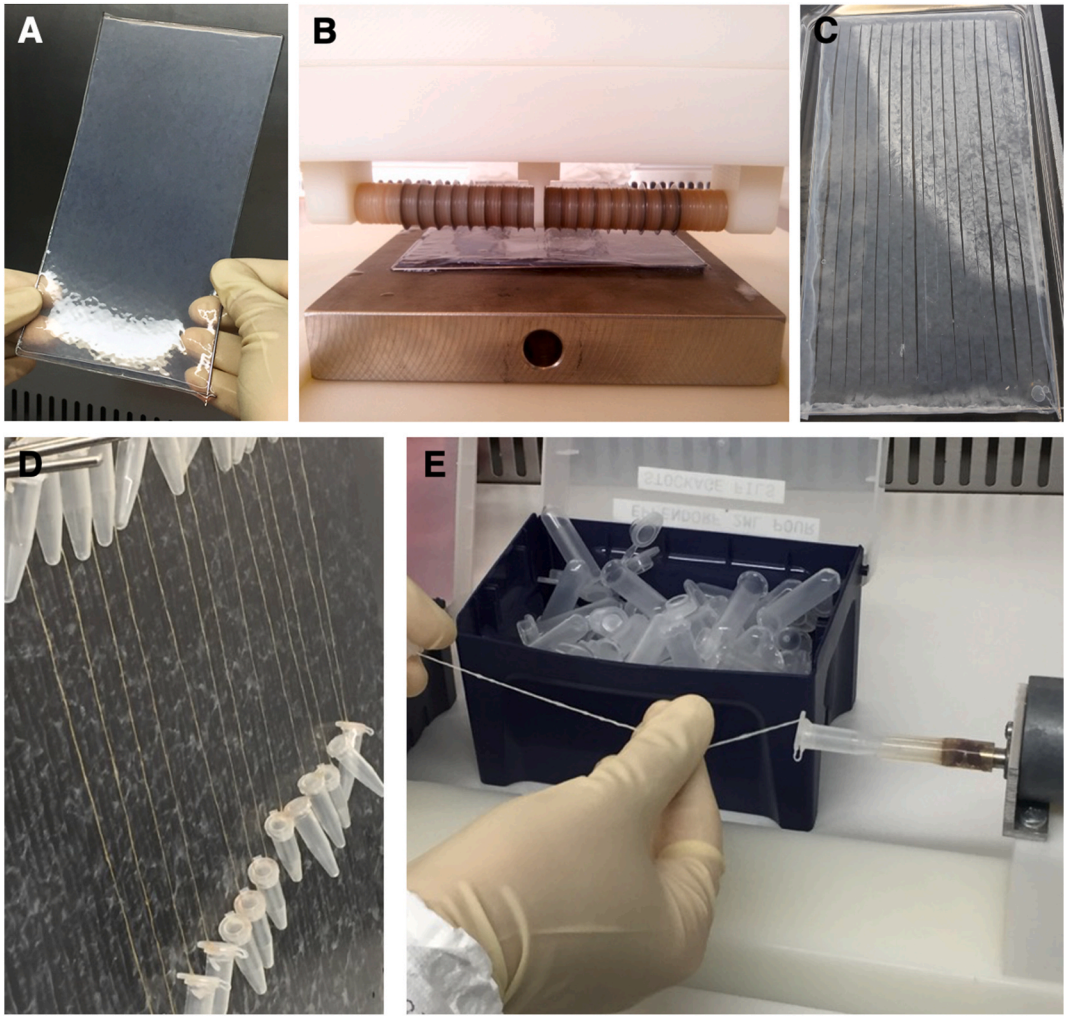

Fig. 1. Sterile yarn manufacturing. (A) Human skin fibroblasts were used to produce 10 × 18 cm^2 sheets of CAM. Sheets were devitalized by dehydration and stored at −80 °C to be available "off-the-shelf". (B–C) To produce ribbons, rehydrated sheets were positioned on the bed of a custom cutting device, and circular blades were used to cut 5-mm wide CAM ribbons. (D) Ribbons were dried under tension in a biosafety cabinet. (E) Twisted yarn (thread) was produced using a custom twisting device where one extremity of the ribbon was attached to the rotation grip of the device, while the other extremity was held by a manipulator. Here, the twisting level was 7.5 revolutions per cm of length.

2.11. Statistical analyses

All statistical analyses were performed with GraphPad Prism, Version 8 (GraphPad Software Inc. USA). Data are presented as mean ± standard deviation (SD). Differences between the groups were determined using two-ways analysis of variance (ANOVA) with Tukey's multiple comparison tests. Differences were considered significant at $P < 0.05$.

3. Results

3.1. Manufacturing of human biological yarns

We have previously taken advantage of the ability of mesenchymal cells to assemble a dense endogenous extracellular matrix (ECM), we call Cell-Assembled Matrix (CAM), when cultured with ascorbate [10–12]. Here, robust sheets of CAM were produced using human skin fibroblasts in 225-cm^2 flasks (Fig. 1A) that can then be cut into ribbons of various width using a multi-blade cutting device (Fig. 1B and C). Ribbons were air-dried under slight tension in a biosafety cabinet to generate a sterile yarn that was spooled and stored at −80 °C (Fig. 1D). Alternatively, ribbons can be twisted to form "threads", which are more compact and have different mechanical properties (Fig. 1E).

3.2. Histological analyses of the yarns after processing

While fresh CAM, containing living cells, can be processed into yarn (Fig. S1), our overall strategy is to produce "off-the-shelf", fully biological, human textiles for regenerative medicine applications. Therefore, we have focused on the use of devitalized CAM (frozen/thawed/dried) that can be stored at −80 °C to maximize manufacturing flexibility. We also studied other processing steps, such as decellularization, gamma sterilization, and twisting, which may be relevant in the manufacturing of textile products. To observe structural changes in processed yarns, we performed histological analyses of cross-sections before implantation (Fig. 2). Devitalized yarns contained cell remnants (dark purple) that could still be clearly identified in the dense collagenous matrix (pink) (Fig. 2A and B). The decellularization process removed all traces of nuclear material and did not affect the staining of the CAM (Fig. 2C and D). Confocal observations coupled with second harmonic generation (SHG) validated the efficacy of the decellularization without affecting the collagenous network (Fig. S2). Conversely, gamma sterilization had a denaturing effect on the CAM (Fig. 2E and F). The dye had a decreased affinity for the collagenous matrix. Moreover, this treatment increased the delamination of the matrix. The twisting process compacted the devitalized CAM and gave a puckered appearance to the CAM (Fig. 2G and H). These data suggest that the devitalization process is a gentle treatment that did not affect the structural integrity of the CAM.

3.3. Subcutaneous implantation of the yarns in a nude rat model

In order to assess both histological and mechanical changes due to *in vivo* remodeling, we subcutaneously implanted long segments of CAM yarns (Fig. 3). The yarns were positioned from the lower back to the upper shoulders of nude rats using a 17 cm-long needle (Fig. 3A and B). The insertion of the needle created a subcutaneous tunnel where the yarn was implanted for two weeks, as well as one, three, and six months.

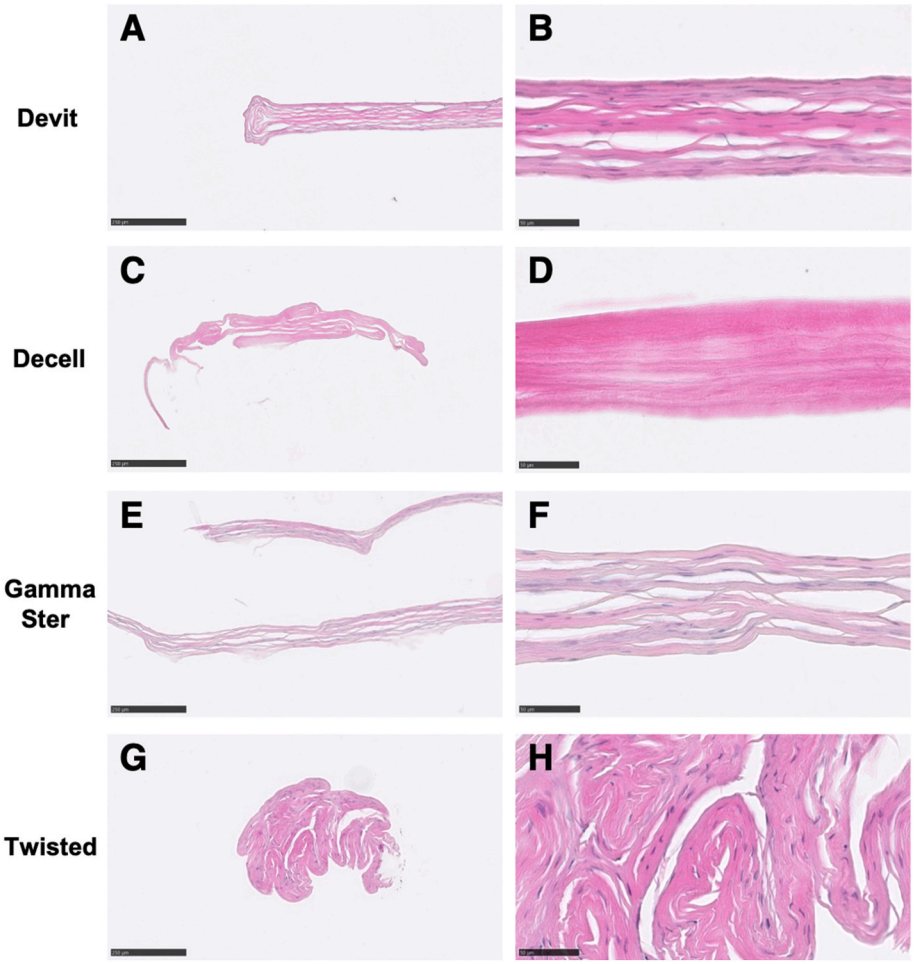

Fig. 2. Histology of biological yarns. (A–H) H&E stained yarn cross-sections before implantation. (A and B) Devitalized yarn (Devit) displayed pycnotic and hyperchromatic nuclei (dark purple), indicative of cell death, embedded in a dense stratified ECM (pink). (C and D) Decellularized yarn (Decell) did not stain for nuclear material, confirming the efficiency of the decellularization process. (E and F) Both matrix and nuclei colorations of the gamma sterilized yarn (Gamma Ster) were reduced compared to their counterparts. (G and H) The twisting process led to the compaction of the tissue and the matrix. Scale bars; 250 μm (left panels) and 50 μm (right panels). (For interpretation of the references to color in this figure legend, the reader is referred to the Web version of this article.)

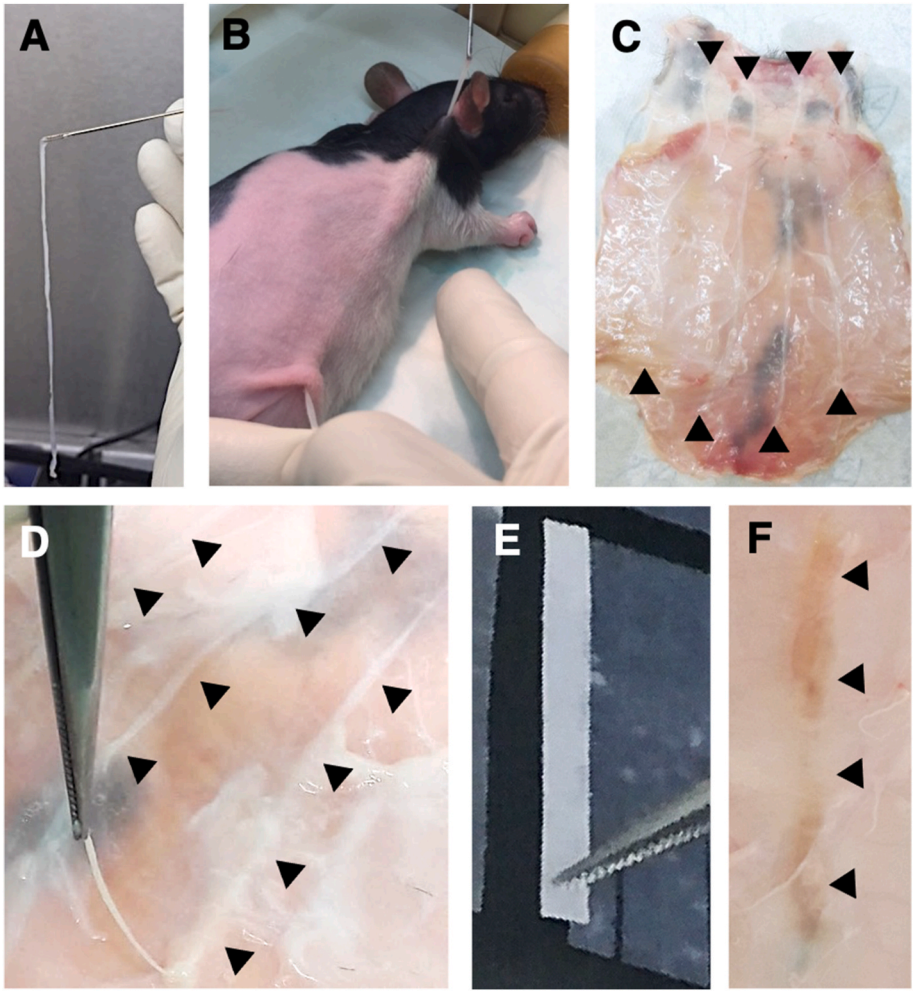

Fig. 3. Subcutaneous implantation in nude rats. (A, B) Yarns were inserted under the skin of the rat using a 17-cm long needle and left for up to six months. (C, D) Yarns were easily identifiable on the underside of the skin six months after implantation (black arrowheads). (E) A strip of a bovine collagen membrane used clinically for oral surgery served as a positive control for innate immune response. (F) After one month, the membrane of processed collagen turned brown (black arrowheads) and was degraded. (For interpretation of the references to color in this figure legend, the reader is referred to the Web version of this article.)

This simple implantation process illustrates how this material can be used just like a suture material [8]. Even six months after implantation, the yarns were easily visible and displayed no macroscopic signs of degradation, inflammation, scarring, or calcification (Fig. 3C). Yarn retrieval was somewhat challenging at longer implantation times because the material was well integrated into the surrounding tissue (Fig. 3D). Great care was taken to only explant the yarn and remove all surrounding tissues. We implanted strips of a commercially available membrane made from purified bovine collagen as a positive control for innate immune reaction (Fig. 3E). After one month of implantation, the membrane was so significantly degraded that it could not be retrieved for mechanical testing. Clearly, it had triggered a strong inflammatory response, as seen by the brown color of the remaining parts of the sample (Fig. 3F; black arrows). This confirmed that nude rats have a functional innate immune system capable of rapidly degrading denatured ECM.

3.4. Histology of devitalized yarn after in vivo remodeling

We then looked at the histology of implanted yarns to evaluate the inflammatory response and *in vivo* remodeling process. At two weeks, devitalized yarns were already well integrated with the surrounding tissue as judged by the close apposition to the native tissue (despite the histological processing), and the presence of migrating fibroblastic cells between and within the CAM layers (Fig. 4A). The fibroblastic nature of these cells was confirmed by immunostaining for type I procollagen (Fig. S3) [13,14]. Fibroblast remnants appeared as dark rounded structures in the CAM. Only mild inflammation was seen at the periphery of the implant, with no inflammatory foci, no giant cells, and no phagocytizing macrophages. Even at this early time point (two weeks), new blood vessels were already observed within the CAM layer (Fig. 4A). By one month, the yarn was tightly connected to the surrounding tissue, colonizing fibroblastic host cells were seen deeper in the implant, blood vessels were seen within the yarn, and some rare immune cells (i.e., rounder cells with a non-fibroblastic phenotype) could still be identified around the tissue (Fig. 4B). No signs of degradation were visible. After three and six months, cell density within the yarn decreased but fibroblastic cells were still present throughout the yarn (Fig. 4C, D and Fig. S4A). The tissue around the yarn appeared as normal loose connective tissue and not a fibrous encapsulation. Vascularization and CAM layer thickness appeared to decrease with time but histological quantification did not show significant differences (Fig. S4B, **C**). Fresh CAM yarns containing living cells underwent a similar *in vivo* remodeling process (Fig. S1A-D). Survival of the human fibroblasts was confirmed by immunostaining for type I procollagen and human-specific nucleoli antigen expression (Fig. S1E,F). In contrast, the purified bovine collagen membrane was completely infiltrated by immune cells after two weeks, and actively phagocytizing macrophages were easily identified throughout the implant site (Fig. 4E). This data indicates that devitalized yarn rapidly integrates in the surrounding tissues with little signs of inflammation unlike denatured collagen. The CAM is colonized, vascularized, and persists for six months in the subcutaneous site in nude rats.

3.5. Histology of processed yarn after in vivo remodeling

Overall, the *in vivo* remodeling was progressive for all yarns with an

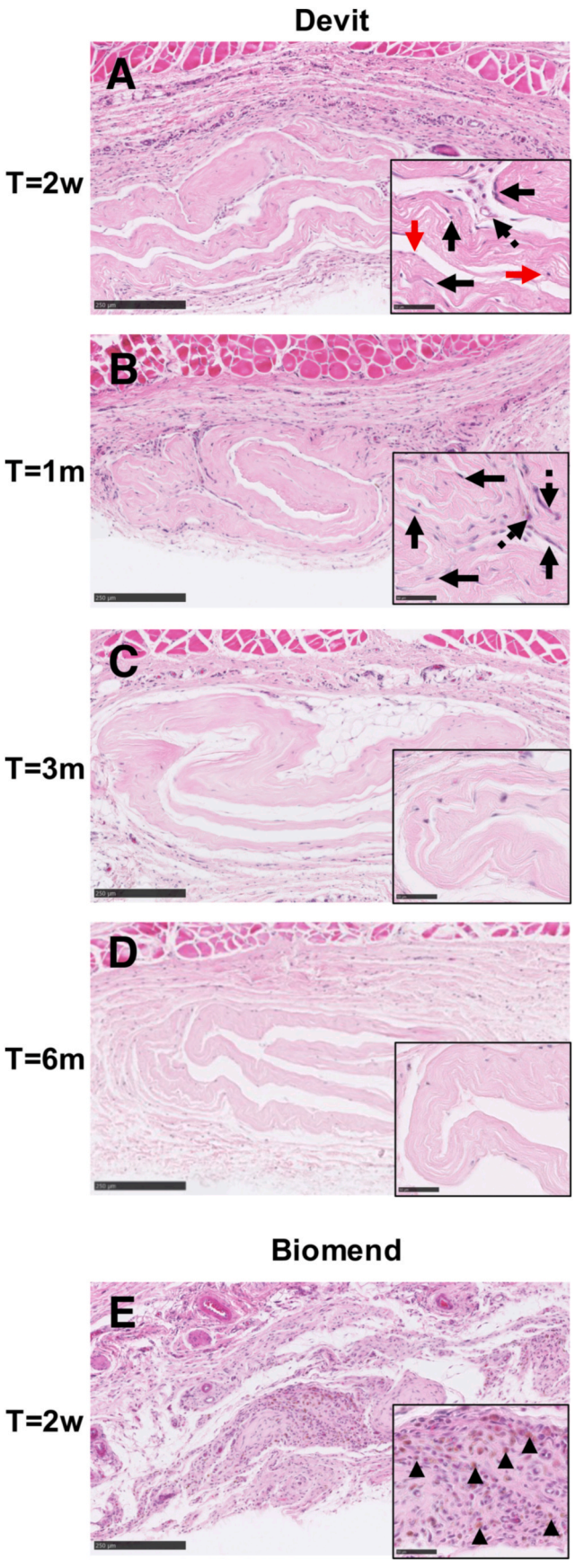

(caption on next column)

Fig. 4. *In vivo* remodeling of devitalized yarn. (A–E) Histological cross-sections at two weeks (T = 2w), as well as one (T = 1 m), three (T = 3 m), and six months (T = 6 m) after subcutaneous implantation in nude rats (H&E). (A) After two weeks, mild inflammation was observed around the devitalized yarns (Devit) and rounded dark cells were seen in the CAM (red arrows). Fibroblastic cells (black arrows) and small blood vessels (dotted lines black arrow) were noted between CAM layers. (B) At one month, fibroblastic cells (black arrows) and vascularization (dotted lines black arrows) were observed. (C, D) By three months and six months, a stable and sparse cell density was achieved with no inflammation or signs of yarn degradation. (E) The commercial collagen membrane (BioMend®) was mostly degraded at two weeks, and brownish, actively phagocytic macrophages were seen at higher magnification (black arrowheads). Scale bars; 250 μm (large panels) and 50 μm (small panels). (For interpretation of the references to color in this figure legend, the reader is referred to the Web version of this article.)

inflammatory response at two weeks that was largely resolved at one month followed by a seemingly stable state at three and six months (Fig. 5 and Fig. S5). After two weeks, host fibroblastic cells were present at the surface of the decellularized yarn and some cells had migrated in the CAM (Fig. 5A and Fig. S4A). Mild inflammation was visible. By six months, the yarn looked like its devitalized counterparts, and blood vessels could occasionally be seen deep in the core of the yarns (Fig. 5B and Fig. S4B). In contrast, at two weeks, gamma sterilized yarns generated a more intense inflammatory reaction with abundant immune cells and blood vessels deep inside the yarn structure, although generally not penetrating the CAM itself (Fig. 5C and Fig. S4B). At six months, the gamma sterilized yarns were sparsely populated with fibroblastic cells lodged in a loose conjunctive tissue and showed reduced signs of inflammation (Fig. 5D and Fig. S4A). The layers of gamma sterilized CAM appeared generally thinner than those of other yarns but this was not confirmed statistically (Fig. 5D and Fig. S4C). The twisting process compacted the CAM which seemed to reduce cell migration in the core of the yarn (Fig. 5E and Fig. S4A). Indeed, accumulations of fibroblastic cells, immune cells, and blood vessels were limited to the periphery of the yarns. However, after six months, the twisted yarn appeared to have unwound as it was much less compact (Fig. 5F). It looked similar to devitalized yarn with a resolved inflammation, sparse fibroblastic cells, and limited vascularization (Fig. S4A, B). These results show that decellularization and twisting of the yarn did not affect its ability to be accepted by the host while gamma sterilization sufficiently modified the CAM to trigger an enhanced inflammatory reaction. However, all yarns appeared well integrated after six months.

3.6. Distribution of three major CAM proteins during in vivo remodeling

To further study the *in vivo* remodeling of the yarns, we analyzed by immunofluorescent staining the distribution of three key ECM proteins previously identified in the CAM [15] (type I collagen, thrombospondin, and fibronectin) (Fig. 6). Type I collagen was homogeneously distributed through the thickness of all yarns, and its distribution did not change over time after implantation (Fig. 6A–H, Fig. S6A-D and Fig. S7A-D). Thrombospondin, which was highly expressed in the CAM before implantation, disappeared after one month of implantation from all yarns except from the gamma sterilized yarns, which, while only faintly stained before implantation, were still stained after six months (Fig. 6I-P, Fig. S6E-H, and Fig. S7E-H). Fibronectin was concentrated on the outer surfaces of the devitalized CAM, presumably where cells were actively growing. The protein was slowly lost over the six months of implantation in all yarns (Fig. 6Q–X, Fig. S6I-L, and Fig. S7I-L). Conversely, gamma sterilized yarns were poorly stained for the fibronectin at T = 2w, but they remained positive over six months of remodeling. This data demonstrates that, independently of the manufacturing process, type I collagen remained abundant within the CAMs over six months of implantation, while thrombospondin and fibronectin proteins were degraded over time.

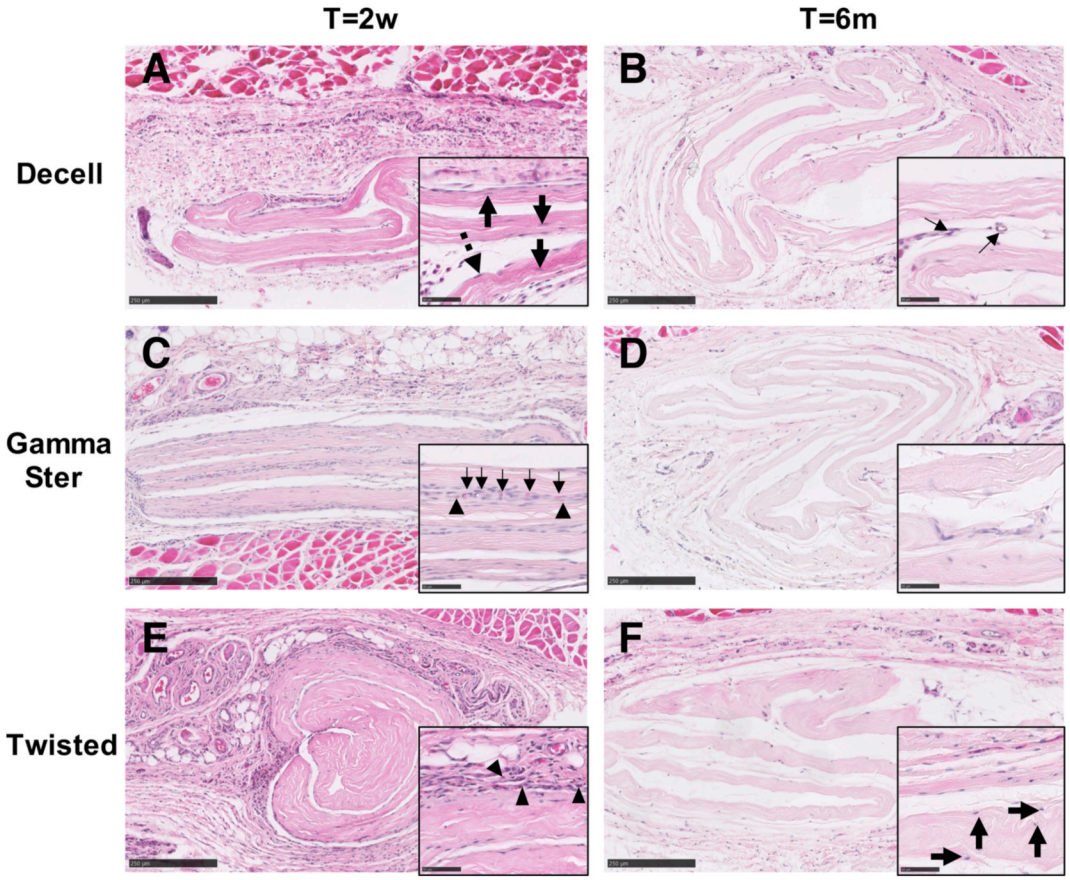

Fig. 5. Impact of processing on yarn *in vivo* remodeling. (A–F) H&E staining of yarn cross-sections at two weeks (T = 2w; left panels) and six months (T = 6 m; right panels) after subcutaneous implantation in nude rats. (A) Decellularized yarns (Decell) were already covered by rat fibroblastic cells after two weeks of implantation and some cells were observed in (black arrows) and on (dotted lines black arrows) the CAM. (B) By six months, the yarn looked like its devitalized counterparts and blood vessels could occasionally be seen deep inside the yarn (small black arrows). (C) After two weeks of implantation, gamma sterilized yarn (Gamma Ster) displayed a more intense inflammatory response with the presence of immune cells (black arrowheads), as well as numerous blood vessels with visible red blood cells (small black arrows). (D) The inflammation had subsided after six months and vascularization was visible (small black arrows). (E) The twisted yarn (Twisted) appeared compact and less colonized by the host's cells after two weeks of implantation. Mild inflammation was observed around the implant (black arrowheads). (F) Yarn were much less compact after six months and were sparsely populated with fibroblastic cells (black arrows). Scale bars; 250 μm (large panels) and 50 μm (small panels). (For interpretation of the references to color in this figure legend, the reader is referred to the Web version of this article.)

3.7. Inflammation response during in vivo remodeling

In order to identify the immune cells observed with basic histology, we quantified M1 (CCR7/CD68 positive cells; inflammation) and M2 (CD206/CD68 positive cells; remodeling) macrophages to analyze the inflammatory response to the various processed yarns (Fig. 7). First, the inflammatory response to fresh and devitalized yarns were compared (Fig. S8). Macrophage density was very low for M1 and M2, and decreased overtime for both yarns (Fig. S8A) showing a very mild inflammatory response to the material. There were no significant differences between the yarns for the density of M1 or M2 macrophages, or their ratios, at any time point (Fig. S8). In a second set of experiments, we compared processed yarns to our "control": the devitalized yarn (Fig. 7). Gamma sterilized yarn showed a statistically higher density of macrophages expressing an inflammatory M1 phenotype than other yarns (Fig. 7Q: Gamma Ster T = 0 vs Devit T = 0, Decell T = 0, and Twisted T = 0: $\#\#P < 0.01$). However, M1 density at the implantation sites of gamma sterilized yarn significantly decreased over time and reached values as low as that of the other yarns at six months, suggesting a resolution of the inflammation (Fig. 7Q: T = 2w vs T = 1 m: $^{**}P < 0.01$; T = 2w vs T = 3 m: $^{****}P < 0.0001$; T = 2w vs T = 6 m: $^{****}P < 0.0001$). M2 macrophages displayed a similar density and decrease over time for all yarns except for the gamma sterilized yarn which was more inflammatory (Fig. 7R: Gamma Ster T = 2w vs T = 6 m: $^{*}P < 0.05$). Finally, M1/M2 ratios did not statistically vary with time or between the yarns (Fig. 7S).

3.8. Mechanical properties of yarns before and after in vivo remodeling

In a first experiment, we implanted fresh yarns containing living cells and devitalized yarns to assess if the devitalization processing would denature the CAM. Samples of around 10-cm long were harvested for each yarn to determine their force at failure and ultimate tensile stress (UTS) after up to six months of *in vivo* remodeling (Fig. S9). No significant differences were observed between fresh and devitalized yarn strength (force at failure) prior or during the six-month-implantation period, which confirmed that the devitalization process did not denature the CAM enough to trigger an innate immune response. Analysis of the UTS showed a drastic increase with longer periods of implantation, which was the result of a decrease in yarn diameters (Fig. S9B). This is suggestive of tissue compaction. We observed a higher variability at later time points (Fig. S9A and B; T = 3 m and T = 6 m). This was attributed to damage caused to yarns during the harvest dissection, which became more challenging as implantation time increased.

In a second experiment, we wanted to examine the effects of additional processing steps that could be relevant for the manufacturing of therapeutic products using biological yarns. These included: active decellularization to remove cellular debris, gamma sterilization, and

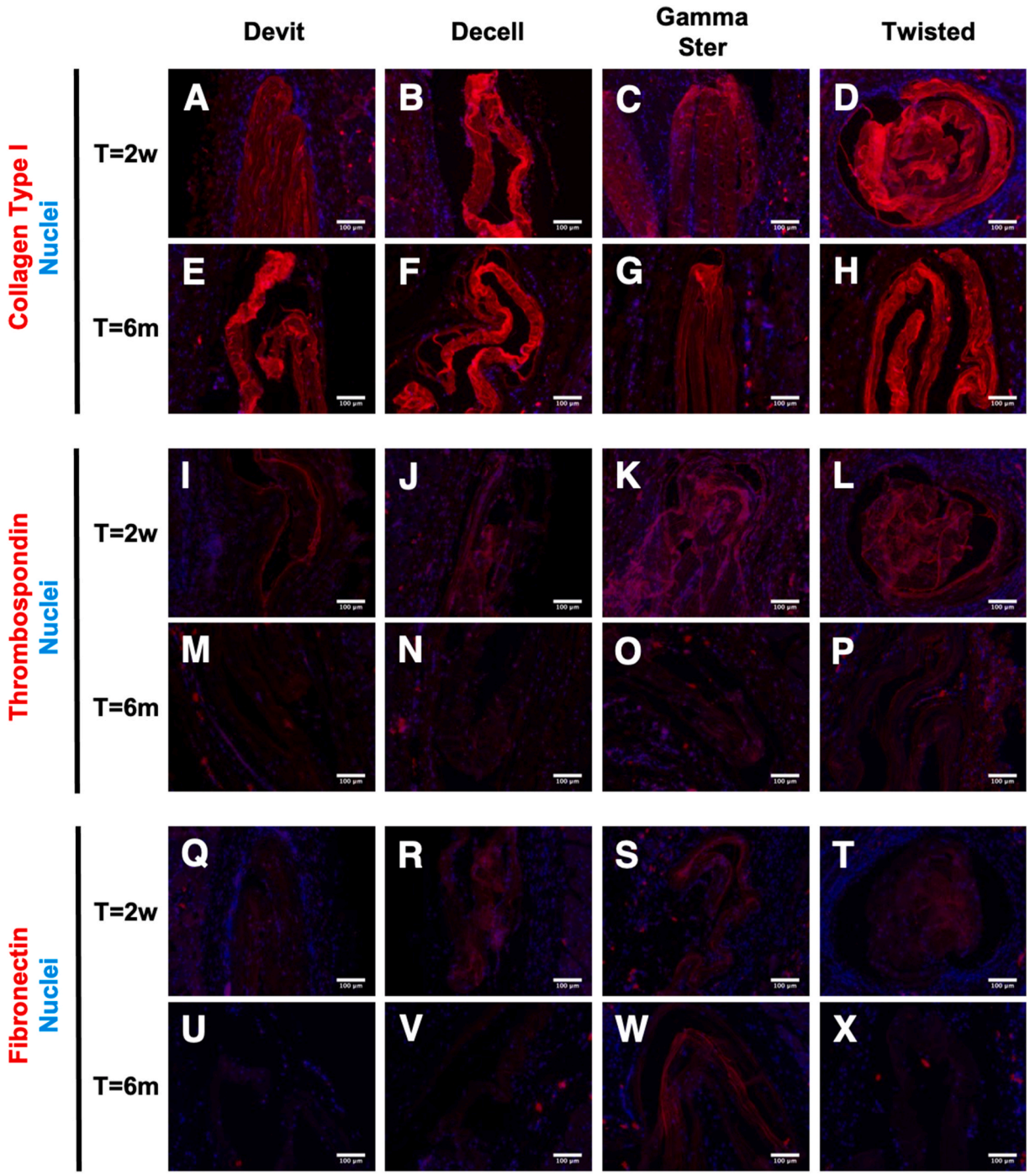

Fig. 6. *In vivo* remodeling of human collagen type I, thrombospondin, and fibronectin in yarns. (A–H) Independently of yarn processing, collagen type I expression (red) appeared unchanged after six months of remodeling (T = 6 m) in nude rats. (I–P) While thrombospondin (red) was expressed within the outer layers of yarns at the early time point of remodeling (T = 2w), it was completely absent from yarns at T = 6 m. (Q–X) Fibronectin (red) was already totally removed from the devitalized yarns, after two weeks of implantation. Scale bars; 100 µm. (For interpretation of the references to color in this figure legend, the reader is referred to the Web version of this article.)

twisting the yarn (Fig. 8). In this experiment, devitalized yarn was used as the reference since this is our preferred form because it allows a simpler manufacturing strategy. We observed lower variability in this experiment probably because we used a less aggressive dissection to avoid damaging yarns. This better resolution allowed the measurement of a statistically significant reduction of the force at failure of devitalized yarn, which occurred within two weeks after implantation (Fig. 8A). However, the strength of the yarn did not further decrease significantly over the next 5.5 months. Prior to implantation (T = 0), we observed that the decellularization process had no effect on yarn strength but this was not the case for gamma sterilization and twisting, which both caused a significant decreased of yarn strength by approximately 25% (Fig. 8A: Devit T = 0 vs Gamma Ster T = 0: $\#\#\#P < 0.001$; Devit T = 0 vs Twisted T = 0: $\#\#\#\#P < 0.0001$). Devitalized, decellularized, and gamma sterilized yarns showed significant reductions of their forces at failure after six months (Fig. 8A: Devit T = 0 vs T = 6 m, Decell T = 0 vs T = 6 m, and Gamma Ster T = 0 vs T = 6 m: $****P < 0.0001$). Like devitalized yarn, decellularized yarn showed an early significant

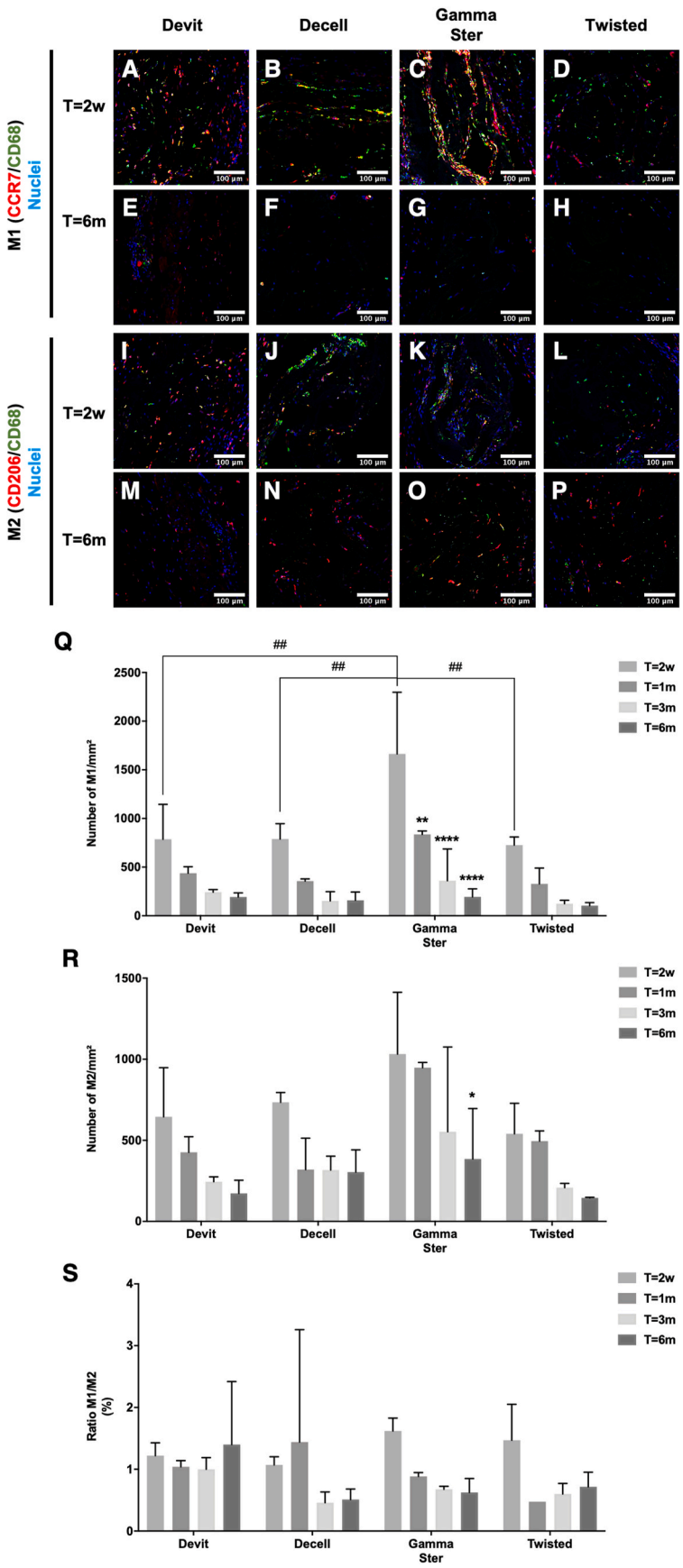

Fig. 7. Macrophages density and phenotype *in vivo* remodeling of the yarns in nude rats. (A–P) M1 macrophages were identified using double immunofluorescent staining against CCR7 (red) and CD68 (green) antigens, while CD206 (red) and CD68 (green) antigens were used for M2 macrophages. Scale bars; 100 µm. (Q) M1 macrophage quantification showed that density decreased over time for all yarns. (R) M2 macrophages quantification showed density levels and a decrease over time that was similar to M1 macrophages. (S) M1/M2 ratios did not statistically vary over time or between yarns. (Significant differences between the T = 2w of each condition: $\#\#P < 0.01$ and significant differences between the T = 2w and other time points within the condition: $^{**}P < 0.01$; $^{****}P < 0.0001$). (For interpretation of the references to color in this figure legend, the reader is referred to the Web version of this article.)

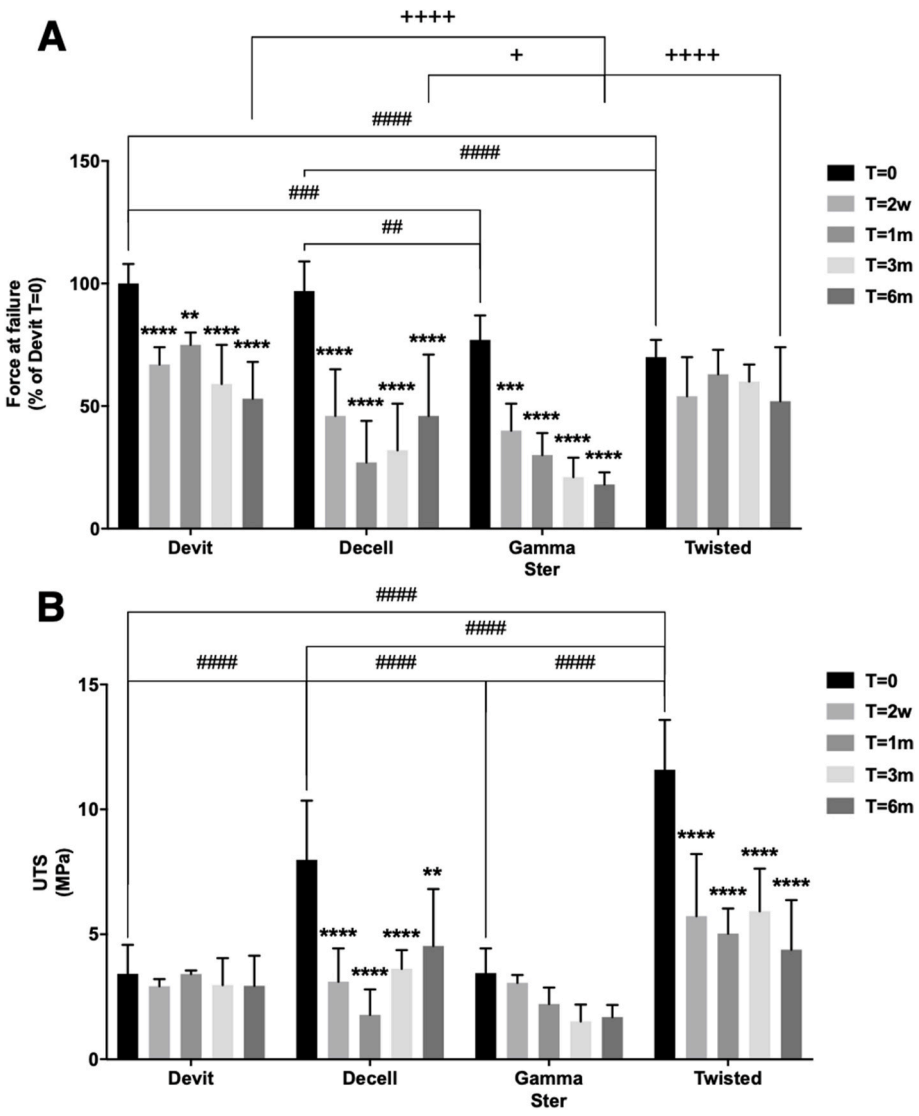

Fig. 8. Evolution of the yarn mechanical properties after *in vivo* remodeling in nude rats for up to six months. (A) Tensile force at failure of yarns as a function of processing and implantation time. (B) Ultimate Tensile Stress (UTS) of yarns as a function of processing and implantation time. UTS evolution was largely guided by force at failure since the diameter did not change at longer time points. (Significant differences between the T = 0 of each condition: $\#\#P < 0.01$; $\#\#\#P < 0.001$; $\#\#\#\#P < 0.0001$, significant differences between the T = 6 m of each condition: $+ P < 0.05$; $++++ P < 0.0001$, and significant differences between the T = 0 and other time points within the condition: $^{**}P < 0.01$; $^{***}P < 0.001$; $^{****}P < 0.0001$).

reduction in strength (Fig. 8A: Decell T = 0 vs T = 2w, T = 1 m, T = 3 m, and T = 6 m: $^{****}P < 0.0001$) with non-significant changes in strength up to the six-month time point. While explanted decellularized yarn tended to be weaker than devitalized yarn, this difference was never statistically significant. Unlike these two yarns, the strength of gamma sterilized yarn seemed to progressively decrease and became significantly weaker than that of devitalized yarn at six months (Fig. 8A: Devit T = 6 m vs Gamma Ster T = 6 m: $++++ P < 0.0001$), which is coherent with the increased inflammatory response observed by histology. Unlike all the other yarns, the much denser twisted yarn did not lose significant mechanical strength at any point after implantation, suggesting that the high compaction of the matrix made it more resistant to early *in vivo* remodeling. Overall, after six months of *in vivo* remodeling, devitalized, decellularized, and twisted yarns showed the same stable force at failure, which was approximately 50% of the initial force of the devitalized yarn at T = 0.

The UTS of the devitalized CAM was 3.4 ± 1.2 MPa and remained constant after implantation. Decellularization of the yarn significantly increased the UTS at T = 0 (Fig. 8B: Devit T = 0 vs Decell T = 0: $\#\#\#\#P < 0.0001$) because it compacted the matrix and resulted in a smaller diameter. However, the UTS of decellularized yarn decreased to devitalized levels within two weeks after implantation (Fig. 8B: Decell T = 0 vs T = 2w: $^{****}P < 0.0001$) largely due to an apparent increase in diameter. UTS then changed with time following the pattern observed for the force at failure (Fig. 8A) because the diameter was stable. Gamma sterilization caused a decrease in yarn diameter resulting in a UTS that was equal to that of non-sterilized devitalized yarn (Fig. 8B). The UTS did not significantly change during the implantation period although it trended down with time like the force at failure. Twisting at 7.5 rev/cm, which is a high level of compaction, tripled the UTS of the yarn (Fig. 8B: Devit T = 0 vs Twisted T = 0: $\#\#\#\#P < 0.0001$). The UTS significantly dropped in the first two weeks of implantation (Fig. 8B: Twisted T = 0 vs T = 2w: $^{****}P < 0.0001$) but remained stable for the remainder of the experiment. These results were driven by an increase in diameter due to the unwinding of the yarn, based on histology results. Taken together, this data shows how different processing can affect yarn mechanical properties and their evolution after *in vivo* implantation.

4. Discussion

Medical textiles have been used in vascular surgery for decades: from simple sutures to complex covered stents [16]. We have previously demonstrated that we can produce completely biological human textiles using yarn of cell-assembled extracellular matrix (CAM) produced in the laboratory [8]. In the context of small-caliber vessels replacement, we have shown that a TEVG produced from woven CAM yarn has mechanical properties that exceed the requirement for *in vivo* implantation. We have previously shown that TEVGs obtained by rolling human CAM

sheets demonstrated promising outcomes as an arteriovenous shunt in patients for over 20 months (up to 36 months, unpublished data) [1,5]. While these clinical results established the long-term *in vivo* persistence of the CAM, they yielded little information on its remodeling process. In this study, we aimed to analyze the CAM remodeling in a much more controlled environment and using a simpler implant to gather both histological and mechanical information. We also wanted to assess how CAM processing could affect its *in vivo* remodeling. Results showed that the CAM yarn caused a very mild inflammatory response that quickly subsided to allow the material to fully integrate and persist in a nude rat model for at least six months.

In this study, immunodeficient rat model was selected to evaluate the innate immune response (inflammation) while avoiding any rejection of xenogeneic material (human CAM) by the adaptive immune system [9,17]. To prove that the nude rat innate immune system was functional, we implanted a clinically available reconstituted collagen membrane and, as expected, this denatured collagen was aggressively degraded. The membrane, which has a predicted life of eight weeks in humans, according to the manufacturer, was already irretrievable two weeks after implantation. In contrast, our human "bio" material (CAM) was easily identified and could be explanted after six months. The subcutaneous space is a standard site for biocompatibility studies (ISO 10993–6:2016) and made possible the implantation and retrieval of long yarn segments. This allowed direct mechanical testing on many, relatively large, samples to provide more direct, and potentially more reliable, data than is possible with miniaturized of indirect measurements strategies that are needed for smaller implants. Nevertheless, the remodeling observed here may not be directly transposable to other implantation sites. In addition, this model does not allow the study of allogeneic immune responses. However, results from our group and others suggest that allogenic responses to tissue-engineered constructs are not significant enough to jeopardize tissue function [2,6,18]. In order to study allogeneic responses, we are developing a large animal model where ovine CAM yarns and TEVGs will be grafted in sheep to assess long-term *in vivo* remodeling (one year).

Mechanically, fresh and devitalized yarns were not significantly different before or after implantation (Fig. S9). This is in agreement with our previous results showing that CAM organization is not substantially affected by the devitalization process [15]. The *in vivo* remodeling of fresh yarns was slightly different as more cells were present at all times (Fig. S1), suggesting that human fibroblastic cells within the CAM can survive implantations. In addition, more blood vessels were observed in the fresh CAM yarns, which may be the consequence of having living mesenchymal cells that secrete paracrine signals (vascular endothelial growth factors or angiopoietins) promoting revascularization after implantation [19,20]. While the *in vivo* remodeling of fresh CAM is interesting, we focused this study on devitalized yarns because they are more compatible with a commercially viable strategy for human textile manufacturing [8]. A key objective of this study was to compare devitalized yarn with yarns that were further processed by either decellularizing the matrix with chemicals, gamma sterilizing, or tightly twisting the ribbon into a compact yarn. These are all relevant processing steps for tissue engineering approaches, since they may reduce the inflammatory response, allow non-sterile yarn production and assembly, or tune the mechanical properties of the yarn, respectively.

Extracellular matrix decellularization has been investigated by several research groups to create "off-the-shelf" tissues or organs for regenerative medicine applications [2,21–26]. Our data demonstrated that decellularized yarns had similar initial mechanical strength and *in vivo* remodeling compared to devitalized ones. While debris from dead cells are often cited as important inflammatory mediators [27,28], this was not observed in our "bio" material based on the histology results and sustained mechanical strength of the yarns. This is consistent with the successful clinical implantation of three allogeneic devitalized CAM-based vascular grafts [6]. This may be because cells died quickly without going into apoptosis or other types of programmed cell death. In addition, the decellularization process did not seem to denature the matrix significantly. While the data suggest that this process does not modify the CAM properties, it appears to be an unnecessary additional step that may create the risk of leaving chemical residues [29].

One of the main challenges in the manufacturing of a biological product is to ensure sterility during its manufacturing. While we have shown that CAM can be produced sterilely under good manufacturing practices (GMP) conditions [1,5,6], terminal sterilization can be a convenient and economical manufacturing step. Gamma irradiation is a widely used sterilization process to guarantee the safety of collagen-based materials [30–32]. In this study, we showed that this treatment affected the CAM by decreasing its mechanical strength, changing its histological appearance, modifying its affinity for stains, and even affecting the remodeling of an important matrix protein (Thrombospondin) (Fig. S6). At the time of implantation, the gamma sterilized yarn even felt different as it was more transparent, stiffer, and more hydrophobic. Consistent with our results, Dearth et al. demonstrated that the gamma sterilization process significantly reduced the mechanical properties (burst strength and suture retention) of porcine dermal ECM scaffold materials, and the impact was dose-dependent [33]. In addition, they also showed that the increase of gamma irradiation dosages elicits an augmented rate of biomaterial degradation following 35 days of implantation in the abdominal walls of rats [33]. It was also demonstrated that it could severely damage collagen fibers, via crosslinking and/or peptide chain scission [34–38]. Similarly, we found that gamma sterilization also influenced the remodeling process as it significantly increased the density of M1 macrophages at early time points (two weeks) in nude rats. Nonetheless, this inflammatory response was resolved after six months, which leaves the possibility of using this process if these changes are taken into account in the product design. Future studies will explore other sterilization methods, such as ethylene oxide, e-beam, supercritical CO_2, or liquid chemicals, in order to identify the least denaturing process for our collagen-based "bio" material.

We also analyzed the *in vivo* remodeling of compacted twisted yarns after implantation. Indeed, this process can be crucial in the production of human textiles in order to tune their mechanical behavior [8]. Interestingly, twisting the CAM yarns decreased the force at failure but significantly increased the UTS of the "bio" material. It also protected it from the initial inflammatory response of the host, which caused a significant early decrease in mechanical strength of all other yarns within the first two weeks. Histological analyses suggested that this was due to tissue compaction that prevented access by inflammatory cells to the core of the CAM at the early time point (two weeks). With time, twisted yarns were less compact on histology, as they probably unwound because of residual tensions in the CAM, but by then, the mild and transient inflammatory response was over.

Quantification of M1/M2 macrophages failed to show significant differences. This was linked to the large variability which was the result of the low macrophage counts combined with the usual animal-to-animal variability. Similar difficulty in achieving significance was also reported by Korzinskas et al. with similarly low macrophage densities [39].

Using a textile-based manufacturing approach, we have demonstrated our ability to use CAM yarns for the production of small diameter woven TEVGs with supraphysiological strength [8]. Such TEVGs could tolerate a significant loss of mechanical strength during their *in vivo* remodeling so the weakening of the CAM after the transient acute inflammation caused by the implantation should not be problematic for their success a vascular conduit. In that same study, we also showed that CAM yarns could be used a suture material to close a wound in a nude rat. Full wound closure and healing was achieved with no macroscopic signs of inflammation. Histological staining after one month confirmed the persistence of the CAM in the skin while it disappeared from the surface of the wound after two weeks. This result is consistent with the *in vivo* behavior observed in the current study and confirms the potential of

CAM-based material for clinical applications.

5. Conclusion

This study was the first formal evaluation of CAM remodeling *in vivo*. At the end of the six-month implantation period, yarns were well integrated in a loose conjunctive tissue with no signs of chronic inflammation (no inflammatory foci, no giant cells, no phagocytizing macrophages or calcification). No dense or acellular fibrous encapsulation was observed. After three months, all yarns were characterized by a sparse population of fibroblastic cells within the CAM and occasional blood vessels. The same observations were made at six months, suggesting a stable remodeling. Taken together, these results demonstrate that the CAM is a long-lived biological material that causes little inflammation and fully integrates in the host after implantation. Consequently, CAM yarns are promising materials to produce completely biological human textiles for various regenerative medicine applications where low inflammatory responses, sustained mechanical strength, or a slow remodeling process are essential.

Credit author statement

Laure Magnan: Conceptualization, Methodology, Software, Validation, Formal analysis, Investigation, Data curation, Writing – original draft, Visualization. **Fabien Kawecki**: Methodolgy, Formal analysis, Data curation, Writing – original draft, Visualization. **Gaëlle Labrunie**: Methodology, Formal analysis, Investigation, Data curation. **Julien Izotte**: Methodology, Investigation, Resources. **Sébastien Marais**: Methodology, Software, Investigation, Resources. **Marie-Pierre Foulc**: Resources, Project administration. **Mickaël Lafourcade**: Methodology, Investigation. **Nicolas L'Heureux**: Conceptualization, Resources, Writing – review & editing, Supervision, Project administration, Funding acquisition.

Declaration of competing interest

The authors declare that they have no known competing financial interests or personal relationships that could have appeared to influence the work reported in this paper.

Acknowledgments

This work was supported by the French "Ministère de la Recherche et de l'Enseignement Supérieur"; the chair senior of the "Initiative d'Excellence de l'Université de Bordeaux (IdEx Bordeaux)" (grant 2016-0389); the French "Agence Nationale de la Recherche (ANR)" (grant number: ANR-16-CE18-0024-01); and the European Research Council (Advanced Grant # 785908). We thank Sylvie Rey, Robin Siadous, Niki Sarika, Yoann Torres, Agathe Grémare, Lionel Couraud, and the "CIC-IT Biomatériaux et dispositifs médicaux implantables" for their technical supports.

Appendix A. Supplementary data

Supplementary data to this article can be found online at https://doi.org/10.1016/j.biomaterials.2021.120815.

References

[1] T.N. McAllister, M. Maruszewski, S.A. Garrido, W. Wystrychowski, N. Dusserre, A. Marini, K. Zagalski, A. Fiorillo, H. Avila, X. Manglano, J. Antonelli, A. Kocher, M. Zembala, L. Cierpka, L.M. de la Fuente, N. L'Heureux, Effectiveness of haemodialysis access with an autologous tissue-engineered vascular graft: a multicentre cohort study, Lancet 373 (2009) 1440–1446, https://doi.org/10.1016/S0140-6736(09)60248-8.

[2] J.H. Lawson, M.H. Glickman, M. Ilzecki, T. Jakimowicz, A. Jaroszynski, E.K. Peden, A.J. Pilgrim, H.L. Prichard, M. Guziewicz, S. Przywara, J. Szmidt, J. Turek, W. Witkiewicz, N. Zapotoczny, T. Zubilewicz, L.E. Niklason, Bioengineered human acellular vessels for dialysis access in patients with end-stage renal disease: two phase 2 single-arm trials, Lancet 387 (2016) 2026–2034, https://doi.org/10.1016/S0140-6736(16)00557-2.

[3] N. L'Heureux, S. Pâquet, R. Labbé, L. Germain, F.A. Auger, A completely biological tissue-engineered human blood vessel, Faseb. J. 12 (1998) 47–56, https://doi.org/10.1096/fasebj.12.1.47.

[4] N. L'Heureux, N. Dusserre, G. Konig, B. Victor, P. Keire, T.N. Wight, N.A. F. Chronos, A.E. Kyles, C.R. Gregory, G. Hoyt, R.C. Robbins, T.N. McAllister, Human tissue-engineered blood vessels for adult arterial revascularization, Nat. Med. 12 (2006) 361–365, https://doi.org/10.1038/nm1364.

[5] N. L'Heureux, T.N. McAllister, L.M. De La Fuente, Tissue-engineered blood vessel for adult arterial revascularization, N. Engl. J. Med. 357 (2007) 1451–1453, https://doi.org/10.1056/NEJMc071536.

[6] W. Wystrychowski, T.N. McAllister, K. Zagalski, N. Dusserre, L. Cierpka, N. L'Heureux, First human use of an allogeneic tissue-engineered vascular graft for hemodialysis access, J. Vasc. Surg. 60 (2014) 1353–1357, https://doi.org/10.1016/j.jvs.2013.08.018.

[7] G. Konig, T.N. McAllister, N. Dusserre, S.A. Garrido, C. Iyican, A. Marini, A. Fiorillo, H. Avila, W. Wystrychowski, K. Zagalski, M. Maruszewski, A.L. Jones, L. Cierpka, L.M. de la Fuente, N. L'Heureux, Mechanical properties of completely autologous human tissue engineered blood vessels compared to human saphenous vein and mammary artery, Biomaterials 30 (2009) 1542–1550, https://doi.org/10.1016/j.biomaterials.2008.11.011.

[8] L. Magnan, G. Labrunie, M. Fénelon, N. Dusserre, M.P. Foulc, M. Lafourcade, I. Svahn, E. Gontier, J.H. Vélez V, T.N. McAllister, N. L'Heureux, Human textiles: a cell-synthesized yarn as a truly "bio" material for tissue engineering applications, Acta Biomater. 105 (2020) 111–120, https://doi.org/10.1016/j.actbio.2020.01.037.

[9] B. Rolstad, The athymic nude rat: an animal experimental model to reveal novel aspects of innate immune responses? Immunol. Rev. 184 (2001) 136–144, https://doi.org/10.1034/j.1600-065x.2001.1840113.x.

[10] J.M. Davidson, P.A. LuValle, O. Zoia, D. Quaglino, M. Giro, Ascorbate differentially regulates elastin and collagen biosynthesis in vascular smooth muscle cells and skin fibroblasts by pretranslational mechanisms, J. Biol. Chem. 272 (1997) 345–352, https://doi.org/10.1074/jbc.272.1.345.

[11] J. Geesin, Regulation of collagen synthesis in human dermal fibroblasts in contracted collagen gels by ascorbic acid, growth factors, and inhibitors of lipid peroxidation, Exp. Cell Res. 206 (1993) 283–290, https://doi.org/10.1006/excr.1993.1148.

[12] D. Chan, S.R. Lamande, W.G. Cole, J.F. Bateman, Regulation of procollagen synthesis and processing during ascorbate-induced extracellular matrix accumulation in vitro, Biochem. J. 269 (1990) 175–181, https://doi.org/10.1042/bj2690175.

[13] C. Reese, R. Lee, M. Bonner, B. Perry, J. Heywood, R.M. Silver M, E. Tourkina, R. P. Visconti, S. Hoffman, Fibrocytes in the fibrotic lung: altered phenotype detected by flow cytometry, Front. Pharmacol. 5 (JUN) (2014) 1–13, https://doi.org/10.3389/fphar.2014.00141.

[14] M.E. Yeager, C.M. Nguyen, D.D. Belchenko, K.L. Colvin, S. Takatsuki, D.D. Ivy, K. R. Stenmark, Circulating fibrocytes are increased in children and young adults with pulmonary hypertension, Eur. Respir. J. 39 (2012) 104–111, https://doi.org/10.1183/09031936.00072311.

[15] L. Magnan, G. Labrunie, S. Marais, S. Rey, N. Dusserre, M. Bonneu, S. Lacomme, E. Gontier, N. L'Heureux, Characterization of a Cell-Assembled extracellular Matrix and the effect of the devitalization process, Acta Biomater. 82 (2018) 56–67, https://doi.org/10.1016/j.actbio.2018.10.006.

[16] C. Singh, C. Wong, X. Wang, Medical textiles as vascular implants and their success to mimic natural arteries, J. Funct. Biomater. 6 (2015) 500–525, https://doi.org/10.3390/jfb6030500.

[17] H.-J. Schuurman, The nude rat, Hum. Exp. Toxicol. 14 (1995) 122–125, https://doi.org/10.1177/096032719501400130.

[18] K.G. Donohue, P. Carson, M. Iriondo, L. Zhou, L. Saap, K. Gibson, V. Falanga, Safety and efficacy of a bilayered skin construct in full-thickness surgical wounds, J. Dermatol. 32 (2005) 626–631, https://doi.org/10.1111/j.1346-8138.2005.tb00811.x.

[19] L. Chen, E.E. Tredget, P.Y.G. Wu, Y. Wu, Paracrine factors of mesenchymal stem cells recruit macrophages and endothelial lineage cells and enhance wound healing, PloS One 3 (2008), e1886, https://doi.org/10.1371/journal.pone.0001886.

[20] J. Rouwkema, N.C. Rivron, C.A. van Blitterswijk, Vascularization in tissue engineering, Trends Biotechnol. 26 (2008) 434–441, https://doi.org/10.1016/j.tibtech.2008.04.009.

[21] Q. Yao, Y.W. Zheng, Q.H. Lan, L. Kou, H.L. Xu, Y.Z. Zhao, Recent development and biomedical applications of decellularized extracellular matrix biomaterials, Mater. Sci. Eng. C 104 (2019) 109942, https://doi.org/10.1016/j.msec.2019.109942.

[22] S. Ilanlou, M. Khakbiz, G. Amoabediny, J. Mohammadi, Preclinical studies of acellular extracellular matrices as small-caliber vascular grafts, Tissue Cell 60 (2019) 25–32, https://doi.org/10.1016/j.tice.2019.07.008.

[23] K.H. Hillebrandt, H. Everwien, N. Haep, E. Keshi, J. Pratschke, I.M. Sauer, Strategies based on organ decellularization and recellularization, Transpl. Int. 32 (2019) 571–585, https://doi.org/10.1111/tri.13462.

[24] C. Quint, Y. Kondo, R.J. Manson, J.H. Lawson, A. Dardik, L.E. Niklason, Decellularized tissue-engineered blood vessel as an arterial conduit, Proc. Natl. Acad. Sci. U. S. A. 108 (2011) 9214–9219, https://doi.org/10.1073/pnas.1019506108.

[25] Z.H. Syedain, M.L. Graham, T.B. Dunn, T. O'Brien, S.L. Johnson, R.J. Schumacher, R.T. Tranquillo, A completely biological "off-the-shelf" arteriovenous graft that

recellularizes in baboons, Sci. Transl. Med. 9 (2017), https://doi.org/10.1126/scitranslmed.aan4209.
[26] Z.H. Syedain, L.A. Meier, M.T. Lahti, S.L. Johnson, R.T. Tranquillo, Implantation of completely biological engineered grafts following decellularization into the sheep femoral artery, Tissue Eng. - Part A. 20 (2014) 1726–1734, https://doi.org/10.1089/ten.tea.2013.0550.
[27] E. Vénéreau, C. Ceriotti, M.E. Bianchi, DAMPs from cell death to new life, Front. Immunol. 6 (2015), https://doi.org/10.3389/fimmu.2015.00422.
[28] J.P. Kolb, T.H. Oguin, A. Oberst, J. Martinez, Programmed cell death and inflammation: winter is coming, Trends Immunol. 38 (2017) 705–718, https://doi.org/10.1016/j.it.2017.06.009.
[29] J. Hwang, B.H. San, N.J. Turner, L.J. White, D.M. Faulk, S.F. Badylak, Y. Li, S. M. Yu, Molecular assessment of collagen denaturation in decellularized tissues using a collagen hybridizing peptide, Acta Biomater. 53 (2017) 268–278, https://doi.org/10.1016/j.actbio.2017.01.079.
[30] S.-S. Gouk, T.-M. Lim, S.-H. Teoh, W.Q. Sun, Alterations of human acellular tissue matrix by gamma irradiation: histology, biomechanical property, stability, in vitro cell repopulation, and remodeling, J. Biomed. Mater. Res. B Appl. Biomater. 84 (2008) 205–217, https://doi.org/10.1002/jbm.b.30862.
[31] M.F. Moreau, Y. Gallois, M.F. Baslé, D. Chappard, Gamma irradiation of human bone allografts alters medullary lipids and releases toxic compounds for osteoblast-like cells, Biomaterials 21 (2000) 369–376, https://doi.org/10.1016/S0142-9612(99)00193-3.
[32] M. Sloff, H.P. Janke, P.K.J.D. De Jonge, D.M. Tiemessen, B.B.M. Kortmann, S. M. Mihaila, P.J. Geutjes, W.F.J. Feitz, E. Oosterwijk, The impact of γ-irradiation and EtO degassing on tissue remodeling of collagen-based hybrid tubular templates, ACS Biomater. Sci. Eng. 4 (2018) 3282–3290, https://doi.org/10.1021/acsbiomaterials.8b00369.
[33] C.L. Dearth, T.J. Keane, C.A. Carruthers, J.E. Reing, L. Huleihel, C.A. Ranallo, E. W. Kollar, S.F. Badylak, The effect of terminal sterilization on the material properties and in vivo remodeling of a porcine dermal biologic scaffold, Acta Biomater. 33 (2016) 78–87, https://doi.org/10.1016/j.actbio.2016.01.038.
[34] D.T. Cheung, N. Perelman, D. Tong, M.E. Nimni, The effect of γ-irradiation on collagen molecules, isolated α-chains, and crosslinked native fibers, J. Biomed. Mater. Res. 24 (1990) 581–589, https://doi.org/10.1002/jbm.820240505.
[35] H.E. Schwartz, M.J. Matava, F.S. Proch, C.A. Butler, A. Ratcliffe, M. Levy, D. L. Butler, The effect of gamma irradiation on anterior cruciate ligament allograft biomechanical and biochemical properties in the caprine model at time zero and at 6 months after surgery, Am. J. Sports Med. 34 (2006) 1747–1755, https://doi.org/10.1177/0363546506288851.
[36] B.P. Conrad, M. Rappé, M. Horodyski, K.W. Farmer, P.A. Indelicato, The effect of sterilization on mechanical properties of soft tissue allografts, Cell Tissue Bank. 14 (2013) 359–366, https://doi.org/10.1007/s10561-012-9340-2.
[37] A.J. Bailey, W.J. Tromans, Effects of ionizing radiation on the ultrastructure of collagen fibrils, Radiat. Res. 23 (1964) 145, https://doi.org/10.2307/3571687.
[38] J.H. Bowes, J.A. Moss, The effect of gamma radiation on collagen, Radiat. Res. 16 (1962) 211, https://doi.org/10.2307/3571153.
[39] T. Korzinskas, O. Jung, R. Smeets, S. Stojanovic, S. Najman, K. Glenske, M. Hahn, S. Wenisch, R. Schnettler, M. Barbeck, In vivo analysis of the biocompatibility and macrophage response of a non-resorbable PTFE membrane for guided bone regeneration, Int. J. Mol. Sci. 19 (2018) 1–12, https://doi.org/10.3390/ijms19102952.